PROCEEDINGS OF SCIENCE

Four- and three-body dynamics in ^{6}Li scattering

Shin Watanabe*
RIKEN, Nishina Center
E-mail: shin.watanabe.vf@riken.jp

Takuma Matsumoto
Department of Physics, Kyushu University
E-mail: matsumoto@phys.kyushu-u.ac.jp

Kazuyuki Ogata
Research Center for Nuclear Physics (RCNP), Osaka University
E-mail: kazuyuki@rcnp.osaka-u.ac.jp

Masanobu Yahiro
Department of Physics, Kyushu University
E-mail: yahiro@phys.kyushu-u.ac.jp

We apply a four-body version of the continuum-discretized coupled-channels method (four-body CDCC) to ^{6}Li elastic scattering and investigate four-body dynamics ($n+p+\alpha+$T, where T is a target). Four-body CDCC reproduces the measured cross sections without introducing any adjustable parameter for ^{6}Li + ^{209}Bi scattering at 24–50 MeV and ^{6}Li + ^{208}Pb scattering at 29–210 MeV. We confirm that ^{6}Li breakup effects are important in a wide energy range, and then focus on the competition between four-body (^{6}Li$+$T$\leftrightarrow n+p+\alpha+$T) and three-body (^{6}Li$+$T$\leftrightarrow d+\alpha+$T) channel-couplings. As an interesting property, we find that ^{6}Li is mainly broken up into two particles d and α, and hardly into three particles n, p and α during scattering. This property is now called "$d\alpha$-dominance". Following the $d\alpha$-dominance, we propose an effective three-body model that simulates four-body CDCC calculations reasonably well.

The 26th International Nuclear Physics Conference
11-16 September, 2016
Adelaide, Australia

*Speaker.

PoS(INPC2016)208

1. Introduction

Projectile breakup is a typical dynamic property of nuclei in a scattering system. A treatment of breakup effects is essential to describe scattering of weakly-bound nuclei. The continuum-discretized coupled-channels method (CDCC) is a fully quantum-mechanical method for treating dynamics among various kinds of channels including breakup (continuum) channels. CDCC was first applied to scattering of deuteron (d) on targets (T) in the $n+p+$T three-body model [1, 2]. The breakup effects are found to be significant in a wide incident-energy range, i.e., $E_{\rm in} \lesssim 700$ MeV [1]. Nowadays, this kind of CDCC, which treats scattering of two-body projectiles, is called "three-body CDCC". Three-body CDCC has been widely applied for describing three-body dynamics and/or for extracting projectile properties; see Ref. [3] for the recent development.

Our interest is now going to four-body dynamics of three-body projectiles such as ^{6}He, ^{6}Li, ^{11}Li, etc. Three-body CDCC has been, therefore, extended to four-body CDCC in which the total system is assumed to be a $N+N+$core$+$T four-body model, where N is a nucleon. The concept of four-body CDCC is the same as that of three-body CDCC. However, in practice, the formulation is not straightforward because it is not easy to prepare three-body continuum states for projectiles before coupled-channel calculations. This problem was first solved [4] by the pseudostate method [5] using the Gaussian expansion method [6]. Four-body CDCC is one of the state-of-the-art calculations in nuclear physics.

At the beginning, four-body CDCC was applied to ^{6}He scattering because it is simpler than any other four-body reaction. A clear difference can be found by comparing with ^{6}Li scattering. ^{6}He is a Borromean nucleus described by the $n+n+\alpha$ model. Therefore, ^{6}He has no bound state in its two-body subsystems and the ground and excited continuum states consist only of three-body configurations. On the other hand, ^{6}Li $(n+p+\alpha)$ has a bound state (d) in the n-p subsystem. Therefore, the ground and excited continuum states consist of both $d\alpha$ two-body and $np\alpha$ three-body configurations. This situation leads to the competition of two types of breakup processes in ^{6}Li scattering:

$$\begin{array}{ll} \text{Four-body breakup process :} & {}^6\text{Li}+\text{T} \to n+p+\alpha+\text{T}, \\ \text{Three-body breakup process :} & {}^6\text{Li}+\text{T} \to d+\alpha+\text{T}. \end{array} \tag{1.1}$$

Four-body dynamics of ^{6}Li scattering is thus richer than that of ^{6}He scattering. The elucidation of four-body dynamics scattering should be performed by four-body CDCC with the explicit inclusion of both the processes.

In the present work, we apply four-body CDCC to ^{6}Li + ^{209}Bi scattering near the Coulomb barrier energy $E_{\rm in} \approx 30$MeV. This scattering system was, in fact, analyzed by three-body CDCC using the $d+\alpha+$T model [7]. It was reported that the renormalization factor is necessary for the optical potentials to reproduce the measured elastic cross sections [8, 9]. This result suggests the importance of explicit treatment of the n-p subsystem. Here, we demonstrate that four-body CDCC describes the measured cross sections without introducing any adjustable parameter. We then investigate which of the four- and three-body breakup processes is important in the present ^{6}Li scattering.

2. Theoretical framework

2.1 Four-body CDCC

We summarize four-body CDCC for ^{6}Li scattering from a target nucleus (T); interested readers are referred to Ref. [3, 10] for further information. Since ^{6}Li is well described by the $n+p+\alpha$ three-body model, we consider the $n+p+\alpha+$T four-body system for ^{6}Li scattering. The scattering state Ψ with the total energy E is governed by the four-body Schrödinger equation:

$$(H-E)\Psi=0, \quad H=K_R+U_n+U_p+U_\alpha+\frac{e^2Z_{\rm Li}Z_{\rm T}}{R}+h_{np\alpha}, \tag{2.1}$$

where K_R stands for the kinetic energy operator with respect to the relative coordinate R between ^{6}Li and T, and U_x ($x=n,p,\alpha$) represents the optical potential between x and T. The Coulomb interactions are approximated into $e^2Z_{\rm Li}Z_{\rm T}/R$ since the Coulomb breakup process has been confirmed to be negligible [7, 10, 12], where $Z_{\rm X}$ is the atomic number of nucleus X. In Eq. (2.1), $h_{np\alpha}$ denotes the internal Hamiltonian of ^{6}Li, the Schrödinger equation for ^{6}Li is then written as

$$(h_{np\alpha}-\varepsilon)\Phi_\varepsilon=0, \quad h_{np\alpha}=K_r+K_y+V_{n\alpha}+V_{p\alpha}+V_{np}, \tag{2.2}$$

where Φ_ε is the ^{6}Li eigenstate with the eigenenergy ε, K_x denotes the kinetic energy operator for the Jacobi coordinate x ($x=r$ or y), and $V_{\rm ab}$ is the interaction between constituent particles a and b.

In CDCC, Eq. (2.1) is solved in the model space P spanned by the ground and discretized-continuum states:

$$P=\sum_{\gamma=0}^{N}|\Phi_\gamma\rangle\langle\Phi_\gamma|, \tag{2.3}$$

where Φ_γ represents the γ-th eigenstate with an eigenenergy ε_γ, i.e., Φ_0 is the ground state and Φ_γ ($\gamma=1$–N) stand for discretized-continuum states. The discretization of continuum states is performed in the pseudostate method [5] with the Gaussian expansion method [6]. This model-space assumption reduces Eq. (2.1) to

$$P(H-E)P\Psi_{\rm CDCC}=0 \tag{2.4}$$

for the CDCC wave function

$$\Psi_{\rm CDCC}=\sum_{\gamma=0}^{N}\chi_\gamma(R)|\Phi_\gamma\rangle, \tag{2.5}$$

where the expansion coefficient χ_γ describes the relative motion between T and ^{6}Li in its γ-th state. Equation (2.4) leads to a set of coupled-channel equations for χ_γ:

$$[K_R+U_{\gamma\gamma}-(E-\varepsilon_\gamma)]\chi_\gamma(R)=-U_{\gamma\gamma'}\chi_{\gamma'}(R) \tag{2.6}$$

with the coupling potentials

$$U_{\gamma\gamma'}=\langle\Phi_\gamma|U_n+U_p+U_\alpha|\Phi_{\gamma'}\rangle+\frac{e^2Z_{\rm Li}Z_{\rm T}}{R}\delta_{\gamma\gamma'}. \tag{2.7}$$

This CDCC equation is solved under the standard boundary condition.

3. Results and Discussion

3.1 Four-body CDCC and three-body CDCC

Elastic scattering of ^{6}Li on a ^{209}Bi target is reanalyzed by four-body CDCC as well as three-body CDCC. The model settings are summarized in Ref. [10, 11, 12]. Figure 1 shows the elastic cross sections as a function of the scattering angle $\theta_{\rm c.m.}$ in the center of mass frame at (a) $E_{\rm in} = 29.9$ MeV and (b) $E_{\rm in} = 32.8$ MeV. The dashed line shows the result of the three-body CDCC calculation, which is almost the same as in the previous study [7]. The three-body CDCC calculation underestimates the experimental data [8, 9], as reported in Ref. [7]. We then apply four-body CDCC in order to explain the discrepancy. As shown by the solid line, the result of the four-body CDCC calculation is in good agreement with the experimental data with no adjustable parameter.

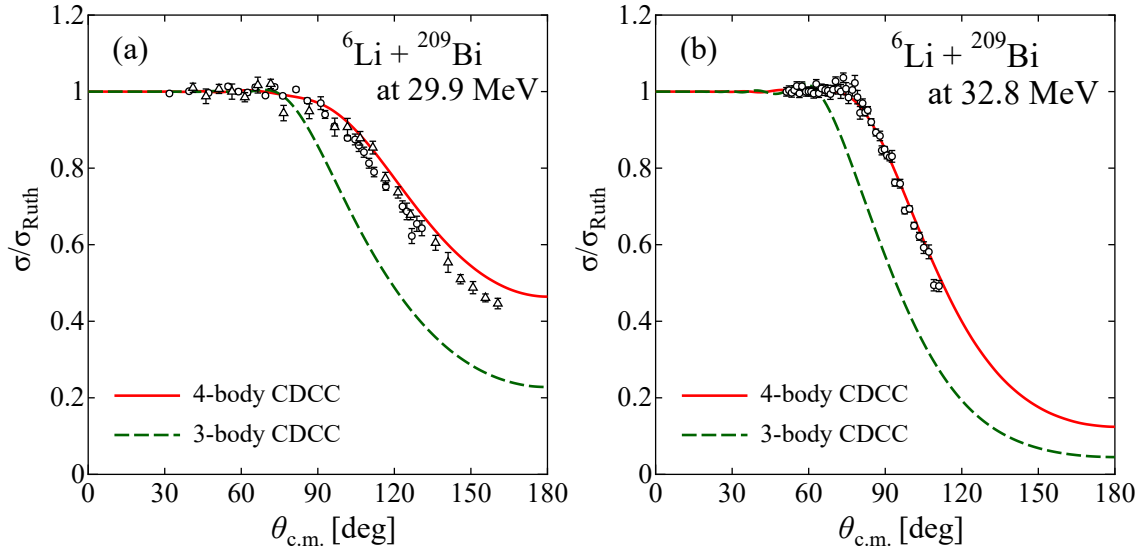

Figure 1: Rutherford ratio of elastic cross sections for ^{6}Li + ^{209}Bi scattering at (a) 29.9 MeV and (b) 32.8 MeV. The solid and dashed lines represent four-body and three-body CDCC calculations, respectively. The experimental data are taken from Ref.[8, 9].

3.2 Four-body breakup mechanism

We also analyze ^{6}Li + ^{208}Pb scattering since the experimental data is available in a wide energy range. In Fig. 2, the elastic cross sections are shown as a function of the transfer momentum (q) for the low (39 MeV) and high (210 MeV) incident energies. Four-body CDCC (solid line) describes the experimental data well as was discussed in Fig. 1, suggesting the reliability of present four-body CDCC. If the breakup effect is neglected, the dotted lines are obtained. We refer to these calculations as full and 1ch calculations, respectively, for the following discussion. The difference between the full and 1ch calculations indicates the importance of breakup channel-coupling effects. The next question to be addressed here is which of the four- and three-body breakup channel is dominant in the present scattering.

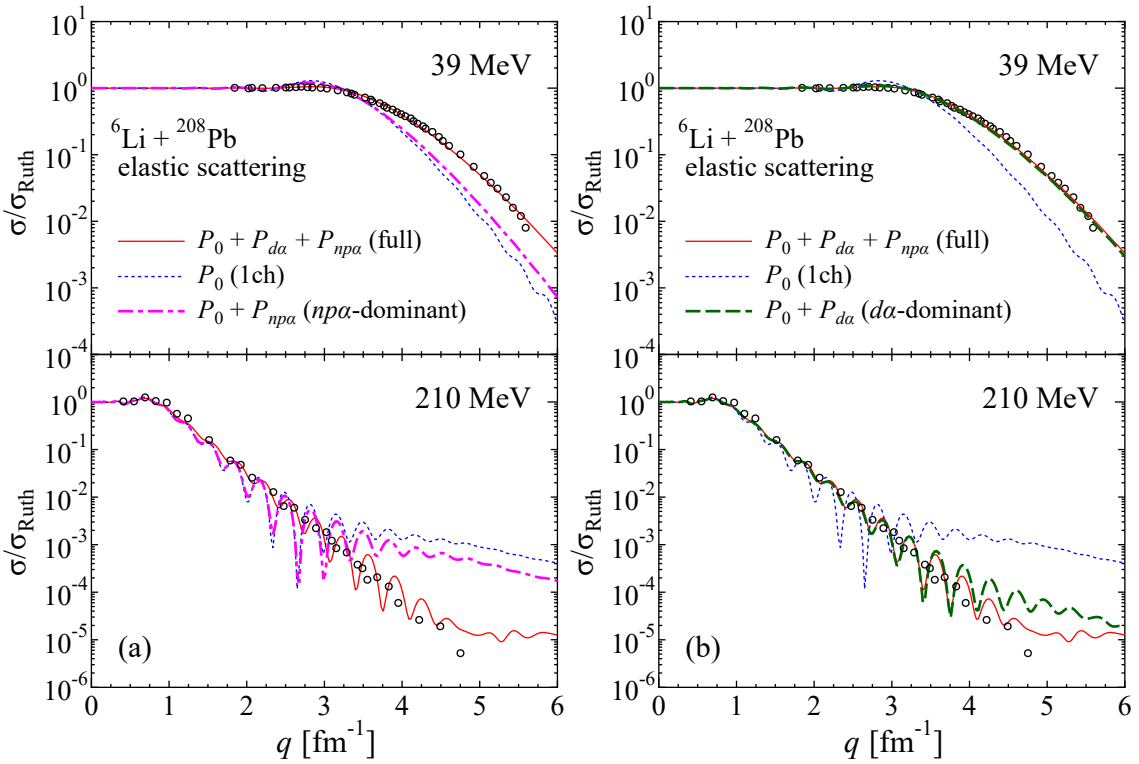

Figure 2: Rutherford ratio of elastic cross sections for ^{6}Li + ^{208}Pb scattering at $E_{\rm in} = 39$ and 210 MeV. The solid and dotted lines represent the results of full and 1ch calculations; note that these lines are the same in (a) and (b). In the dot-dashed line (a), the model space is limited to $P_0 + P_{np\alpha}$, whereas in the dashed line (b), the model space is restricted to $P_0 + P_{d\alpha}$. The experimental data are taken from Refs. [13, 14].

In order to disentangle breakup mechanism of ^{6}Li scattering, we consider coupling effects of four- and three-body breakup channels on elastic channel:

$$\begin{aligned} &\text{Four-body channel-coupling}: \quad {}^6\text{Li} + \text{T} \leftrightarrow n + p + \alpha + \text{T}, \\ &\text{Three-body channel-coupling}: \quad {}^6\text{Li} + \text{T} \leftrightarrow d + \alpha + \text{T}. \end{aligned} \tag{3.1}$$

The definitions of four- and three-body channels are given below. In principle, the three-body ^{6}Li wave function of Eq. (2.2) can be expanded in terms of the ground and excited states of deuteron $\{\phi^{(d)}, \phi^{(d^*)}, \cdots\}$:

$$\Phi_\gamma = \phi^{(d)} \psi_\gamma^{(d)} + \phi^{(d^*)} \psi_\gamma^{(d^*)} + \cdots, \tag{3.2}$$

where the expansion coefficients ψ describe the relative motion between α and d in its ground (d) and excited states (d^*). As seen in Eq. (3.2), the states of ^{6}Li are composed of both $d\alpha$ (two-body) and $np\alpha$ (three-body) configurations. We first derive the probability of $d\alpha$ configurations ($d\alpha$-probability) for each Φ_γ state by taking the overlap between Φ_γ and the d ground state $\phi^{(d)}$: $\Gamma_\gamma^{(d\alpha)} = \left|\langle \phi^{(d)}(y_3) | \Phi_\gamma(y_3, r_3) \rangle\right|^2$. Second, we define $d\alpha$- and $np\alpha$-dominant states as

$$\begin{aligned} &d\alpha\text{-dominant state } |\Phi_\gamma^{(d\alpha)}\rangle: \quad |\Phi_\gamma\rangle \text{ with } \Gamma_\gamma^{(d\alpha)} > 0.5, \\ &np\alpha\text{-dominant state } |\Phi_\gamma^{(np\alpha)}\rangle: \quad |\Phi_\gamma\rangle \text{ with } \Gamma_\gamma^{(d\alpha)} \leq 0.5. \end{aligned} \tag{3.3}$$

In Fig. 3, the $d\alpha$-probabilities are plotted as a function of ε for all the states in the present model space. For example, for the ground state of ^{6}Li, the $d\alpha$-probability obtained is $\Gamma_0^{(d\alpha)} = 0.70$, and the spectroscopic overlap is given by $(\Gamma_0^{(d\alpha)})^{1/2} = 0.83$. This is consistent with the value 0.86 of the other three-body calculation [15] and the experimental estimation 0.85 ± 0.04 [16]. Below the $n+p+\alpha$ threshold energy ($\varepsilon_{\rm th}^{(np\alpha)} = 0$ MeV), all the breakup states are obtained as $d\alpha$-dominant states. Above $\varepsilon_{\rm th}^{(np\alpha)}$, most of the states are $np\alpha$-dominant states and few states are $d\alpha$-dominant ones. The numbers of $np\alpha$- and $d\alpha$-dominant states are 140 and 15 above the $d+\alpha$ threshold energy ($\varepsilon_{\rm th}^{(d\alpha)} = -2.2$ MeV), respectively. This is natural because the three-body phase space is much larger than the two-body one.

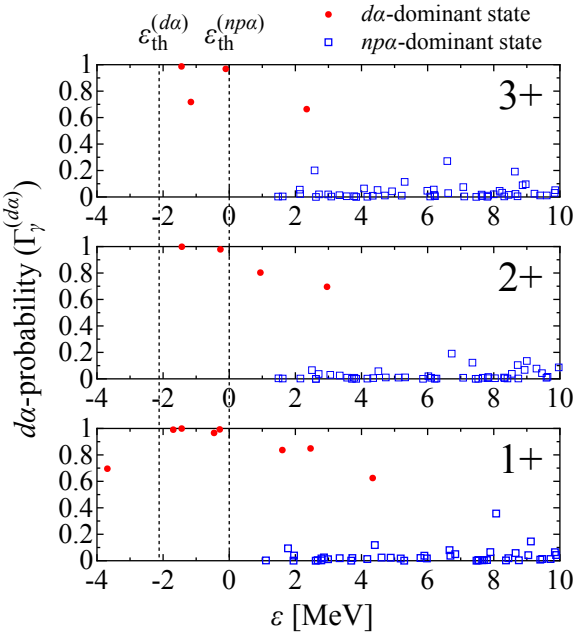

Figure 3: $d\alpha$-probability for states of ^{6}Li. The closed circles (open squares) correspond to the $d\alpha$-dominant states ($np\alpha$-dominant states); see the text for the detail. The threshold energies of $\varepsilon_{\rm th}^{(d\alpha)} = -2.2$ MeV and $\varepsilon_{\rm th}^{(np\alpha)} = 0$ MeV are also shown as the dotted line for reference.

With the $d\alpha$- and $np\alpha$-dominant states classified above, the model space $P = \sum_{\gamma=0}^{N} |\Phi_\gamma\rangle\langle\Phi_\gamma|$ can be decomposed in the following way. First, P is decomposed into the ground-state part $P_0 = |\Phi_0\rangle\langle\Phi_0|$ and the breakup-state part $P^* = \sum_{\gamma=1}^{N} |\Phi_\gamma\rangle\langle\Phi_\gamma|$. The P^* is further separated into the $d\alpha$-dominant part $P_{d\alpha}$ and the $np\alpha$-dominant part $P_{np\alpha}$. The model space P is then

$$P = P_0 + P_{d\alpha} + P_{np\alpha} \tag{3.4}$$

with

$$P_0 = |\Phi_0\rangle\langle\Phi_0|, \quad P_{d\alpha} = \sum_\beta |\Phi_\beta^{(d\alpha)}\rangle\langle\Phi_\beta^{(d\alpha)}|, \quad P_{np\alpha} = \sum_\delta |\Phi_\delta^{(np\alpha)}\rangle\langle\Phi_\delta^{(np\alpha)}|. \tag{3.5}$$

Now, we consider coupling effects of four- and three-body channels on the elastic channel. Again, we focus on ^{6}Li + ^{208}Pb scattering in Fig. 2. The solid and dotted lines denote the results of full and 1ch calculations; they are nothing but CDCC calculations of P and P_0, respectively. For the dot-dashed line in Fig. 2(a), the model space is imposed to $P_0 + P_{np\alpha}$. The result differs little from the 1ch calculation (dotted line). On the other hand, the CDCC calculation of $P_0 + P_{d\alpha}$ simulates the full calculation (solid line) reasonably well for both the incident energies, as shown by the dashed line in Fig. 2(b). This result suggests that ^{6}Li is mainly broken up into $d+\alpha$ and

hardly into $n+p+\alpha$ during the scattering. We refer to this property as *$d\alpha$-dominance* and found that the $d\alpha$-dominance is realized in the present energy range up to $E_{\rm in} = 210$ MeV.

3.3 Effective $d+\alpha+$T three-body model

Finally, we propose an effective $d+\alpha+$T three-body model that reasonably simulates the full four-body CDCC calculation. As the discussion mentioned above, the $d\alpha$-dominance is realized in ^{6}Li scattering, suggesting that the $n+p$ subsystem in ^{6}Li hardly breaks up during the scattering. It is quite different from $d(=n+p)$ scattering in which d-breakup effects are significant up to $E_{\rm in} = 700$ MeV [1]. In three-body CDCC calculations for ^{6}Li scattering, the d-optical potential $U_d^{\rm OP}$ is usually taken. However, the $d\alpha$-dominance indicates that the $U_d^{\rm OP}$, which includes d-breakup effects implicitly, should be replaced by the single folding potential $U_d^{\rm SF}$ defined by $U_d^{\rm SF} = \left\langle \phi^{(d)} \middle| U_n + U_p \middle| \phi^{(d)} \right\rangle$, where $\phi^{(d)}$ stands for the d ground state. Note that the $U_d^{\rm SF}$ never includes d-breakup effects.

Figure 4 shows the validity of the effective $d+\alpha+$T three-body model for ^{6}Li + ^{209}Bi scattering at (a) 29.9 MeV and (b) 32.8 MeV. The solid line corresponds to full four-body CDCC calculations, whereas the dashed and dot-dashed lines represent three-body CDCC calculations with $U_d^{\rm OP}$ and $U_d^{\rm SF}$, respectively. Three-body CDCC calculations with $U_d^{\rm SF}$ simulate the results of four-body CDCC calculations reasonably well. The failure of the traditional three-body CDCC with $U_d^{\rm OP}$ comes form overrating the d-breakup effects which are almost absent in ^{6}Li scattering. The model proposed here is much easier than four-body CDCC and hence quite useful.

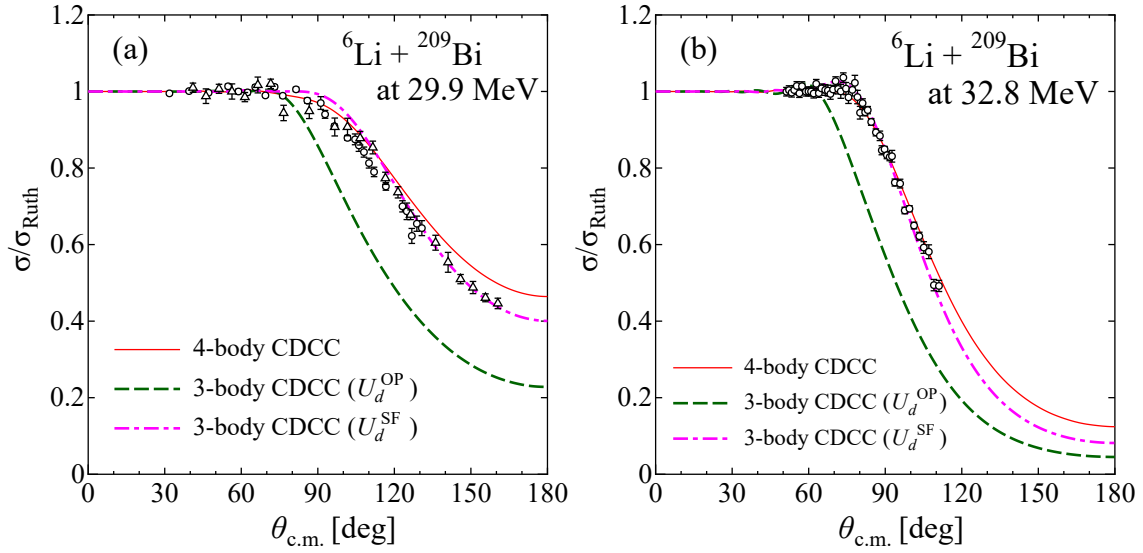

Figure 4: Same as Fig 1, but the results of three-body CDCC calculations with $U_d^{\rm SF}$ are plotted by the dot-dashed line.

4. Summary

Four-body dynamics ($n+p+\alpha+$T) of ^{6}Li elastic scattering has been analyzed in the framework of four-body CDCC. Four-body CDCC has reproduced elastic cross sections for ^{6}Li + ^{209}Bi scattering at $E_{\rm in} = 24$–50 MeV and ^{6}Li + ^{208}Pb scattering at $E_{\rm in} = 29$–210 MeV without introducing

any adjustable parameter. ^{6}Li elastic scattering on heavy targets are thus described by four-body CDCC.

Four-body breakup mechanisms has been investigated. The coupling between elastic and three-body channels is strong, whereas the coupling between elastic and four-body channels is negligibly weak, suggesting that ^{6}Li is mainly broken up into $d+\alpha$ and hardly into $n+p+\alpha$. This property is now referred to as *$d\alpha$-dominance* and confirmed to be realized in a wide energy range. The $d\alpha$-dominance should be a key mechanism of ^{6}Li scattering.

Following the $d\alpha$-dominance, we have proposed an effective three-body model that simulates full four-body CDCC calculations. In the model, the single folding potential $U_d^{\rm SF}$, which can be obtained by folding U_n and U_p with the d ground state, is taken as a potential between d and T. The three-body model with $U_d^{\rm SF}$ simulates the results of four-body CDCC very well. The effective three-body CDCC is much easier than four-body CDCC and hence quite useful.

References

[1] M. Kamimura *et al.*, Prog. Theor. Phys. Suppl. **89**, 1 (1986).

[2] N. Austern *et al.*, Phys. Rep. **154**, 125 (1987).

[3] M. Yahiro *et al.*, Prog. Theor. Exp. Phys. **2012**, 01A206 (2012).

[4] T. Matsumoto *et al.*, Phys. Rev. C **70**, 061601(R) (2004).

[5] T. Matsumoto *et al.*, Phys. Rev. C **68**, 064607 (2003).

[6] E. Hiyama, Y. Kino, and M. Kamimura, Prog. Part. Nucl. Phys. **51**, 223 (2003).

[7] N. Keeley *et al.*, Phys. Rev. C **68**, 054601 (2003).

[8] E. F. Aguilera *et al.*, Phys. Rev. Lett. **84**, 5058 (2000).

[9] E. F. Aguilera *et al.*, Phys. Rev. C **63**, 061603 (2001).

[10] S. Watanabe, Dynamic and Static Properties of Weakly-bound Nuclei, Ph.D. thesis of Kyushu University (2016). http://catalog.lib.kyushu-u.ac.jp/en/recordID/1654646

[11] S. Watanabe *et al.*, Phys. Rev. C **86**, 031601(R) (2012).

[12] S. Watanabe *et al.*, Phys. Rev. C **92**, 044611 (2015).

[13] N. Keeley *et al.*, Nucl. Phys. A **571**, 326 (1994).

[14] A. Nadasen *et al.*, Phys. Rev. C **39**, 536 (1989).

[15] Y. Kikuchi *et al.*, Phys. Rev. C **84**, 064610 (2011).

[16] D. R. Tilley *et al.*, Nucl. Phys. A **708**, 3 (2002).